Microwave-assisted synthesis and characterization of new cathodic material for solid oxide fuel cells: $La_{0.3}Ca_{0.7}Fe_{0.7}Cr_{0.3}O_{3-\delta}$

Beatriz Molero-Sánchez[a], Jesús Prado-Gonjal[b], David Ávila-Brande[b], Viola Birss[a], Emilio Morán[b,*]

[a]*Department of Chemistry, University of Calgary, Calgary, AB, Canada T2N 1N4*
[b]*Universidad Complutense de Madrid, Facultad de Ciencias Químicas, Departamento de Química Inorgánica, 28040 Madrid, Spain*

Abstract

In this work, we examine the benefits of alternative powder processing methods, with a primary focus on microwave-based synthesis, that could both lower material manufacturing costs and further enhance cathode performance for solid oxide fuel cell applications. $La_{0.3}Ca_{0.7}Fe_{0.7}Cr_{0.3}O_{3-\delta}$ (LCFCr), formed using conventional solid-state methods, has been shown in earlier work to be a very promising catalyst for the oxygen reduction reaction. To further increase its performance, microwave methods were used to increase the surface area of LCFCr and to decrease the synthesis time. It was found that the material could be obtained in crystalline form in only 7 h, with the synthesis temperature lowered by roughly 300 °C as compared to conventional methods.

Keywords: Microwave synthesis; Mixed conducting oxides; $La_{0.3}Ca_{0.7}Fe_{0.7}Cr_{0.3}O_{3-\delta}$; HRTEM; Electrocatalysis

1. Introduction

Current research in the solid oxide fuel cell (SOFC) field is moving towards the use of mixed ionic and electronic conducting oxides (MIEC), which have been shown to be more durable as cathodes than conventional $La_{1-x}Sr_xMnO_3$ (LSM) materials. Usually, MIECs are synthesized by solid-state reactions, where the process involves multiple heating (≥ 1200 °C) and regrinding steps to help overcome the solid-state diffusion barrier [1,2]. Some of the methods by which MIECs have been traditionally prepared include the sol–gel method [3], the EDTA citrate complexing process [4], the auto-ignition process [5], the Pechini method [6], and most commonly, by using combustion methods [7].

In order to enhance the diffusion rate of the ceramic precursors by several orders of magnitude, thus shortening the reaction time and potentially lowering the reaction temperature, there has been an interest in the use of microwave-assisted methods. Also, microwave-assisted techniques are understood to be environmentally friendly, as they require less energy than conventional material processing methods. This makes microwave synthesis an example of "Green Chemistry" or "Sustainable Chemistry" [8,9].

The main features that distinguish microwave synthesis from conventional methods are faster energy transfer rates, i.e., more rapid heating rates, and the selective heating of materials. This leads to a unique temperature distribution within the material when it is heated in a microwave furnace. During conventional heat treatment, energy is transferred to a material through thermal conduction and convection, creating thermal gradients. However, in the case of microwave heating, energy is transferred directly to the material through an interaction of the electromagnetic waves with the material at the molecular level [10]. The most important contribution in microwave heating may be that the dipoles in the material follow the alternating electromagnetic field associated with the microwave, with its rapidly changing electric field (ca. 2.4×10^9 times s^{-1}). The resistance to this movement generates a considerable amount of heat [11,12], thus leading to more rapid heating rates.

*Corresponding author.
E-mail address: emoran@quim.ucm.es (E. Morán).

It has been suggested that the more complex a material is, the more difficult it is to prepare using microwave-assisted synthesis. In more complex systems, very good diffusion is required to uniformly disperse three or more cations throughout the sample during the synthesis. The usual solution to this problem is to combine microwave irradiation with other methods, such as sol–gel or combustion synthesis, as has been done for the synthesis of complex perovskites, such as $La_{0.8}Sr_{0.2}Fe_{0.5}Co_{0.5}O_3$ or $CaCu_3Ti_4O_{12}$ [1,13].

Previous research in our group has focused on the development of a sulphur and coke tolerant electrode-supported SOFCs, most recently based on $La_{0.3}Sr_{0.7}Fe_{0.7}Cr_{0.3}O_{3-\delta}$ (LSFCr) as a mixed ionic–electronic conducting perovskite material. LSFCr has shown very good catalytic activity for both H_2/CO oxidation and O_2 reduction, thus potentially having use in symmetrical SOFCs [7]. In order to take advantage of the excellent performance of LSFCr, the A-site of the perovskite was doped with Ca instead of Sr, as Ca has a smaller ionic radius than Sr. The goal was to decrease the thermal expansion coefficient of this derivative of LSFCr, i.e., $La_{0.3}Ca_{0.7}Fe_{0.7}Cr_{0.3}O_{3-\delta}$ (LCFCr), to more closely match that of a Gd-doped ceria (GDC) electrolyte. The partial substitution of Ca for Sr may also enable the introduction of structural inhomogeneties, as Ca doping of $LaFeO_3$ is known to promote oxygen-vacancy ordering [14,15].

In the present study, we are focused on the synthesis and characterization of LCFCr, formed using three different methods, regular combustion (Method 1), microwave-assisted combustion (Method 2), and microwave-assisted sol–gel synthesis (Method 3). We show that a single phase material can be successfully synthesized using microwave-assisted methods and that we can also lower the calcination temperature by 200–300 °C using this approach. Our recent work on LCFCr, synthesized using Method 1, has shown very good electrochemical characteristics [16]. For this reason, parallel comparison studies [17] of the performance of LCFCr-based cathodes, constructed using the three methods described in this paper, are currently being carried out.

2. Experimental methods

2.1. Material synthesis

$La_{0.3}Ca_{0.7}Cr_{0.3}Fe_{0.7}O_{3-\delta}$ (LCFCr) powders were synthesized using three different methods, the regular combustion method (Method 1), microwave-assisted combustion (Method 2), and microwave-assisted sol–gel synthesis (Method 3). When synthesized using the regular combustion method (Method 1), the metal nitrates were mixed in stoichiometric proportions and dissolved in deionized water. A 2:1 mole ratio of glycine to the total cation content was used. Solutions were slowly stirred on a hot plate until auto-ignition and self-sustaining combustion occurred. The sample was first ground and then calcined in air at 1200 °C for 12 h.

LCFCr powders were also synthesized by microwave-assisted combustion (Method 2). Here, the metal nitrates and glycine were dissolved in deionized water using the metal cation proportions required to generate the correct oxide stoichiometry. A 2:1 mole ratio of glycine to the total metal content was used. The stirred solutions were introduced into the microwave furnace and exposed to a 2.45 GHz frequency and 800 W power for 30 min. When the water had evaporated, combustion occurred. The sample was ground and then different fractions were calcined in air at 700 °C, 900 °C and 1000 °C, respectively, for 6 h in order to decompose the organic remnants, rendering a black powder as the final product. The reason for selecting those temperatures is to find the minimum temperature at which the pure phase is formed.

In Method 3, microwave energy and a sol–gel methodology were combined to produce the LCFCr powders, with the metal cation proportions used based on the desired stoichiometry. Metal nitrates were dissolved in distilled water and a saturated polyvinyl alcohol (PVA) solution was added to serve as the complexing agent. The amount of PVA added was such that the ratio of the total number of moles of cations to that of PVA was 1:2. Then the final solution was maintained at 80 °C for 1.5 h to form a viscous gel. The gel was then microwave irradiated (up to 30 min) in a porcelain crucible placed inside another larger crucible filled with mullite. The microwave source was again operated at a 2.45 GHz frequency and 800 W power. Fractions of the polymeric precursor were first ground and then calcined in air at 700 °C, 900 °C and 1000 °C, respectively, for 6 h in order to decompose the organic remnants, rendering a black powder as the final product.

2.2. Material characterization

X-ray diffraction (XRD) patterns of all samples synthesized in this work were collected using a Philips X'Pert PRO ALPHA1 of Panalytical B.V. diffractometer with Cu $K_{\alpha 1}$ monochromatic radiation ($\lambda = 1.54056$ Å). The diffractometer was equipped with a primary curved Ge111 primary beam monochromator and a speed X'Celerator fast detector, operating at 45 kV and 40 mA. XRD patterns were collected in the 2θ range of 5–120° at room temperature, with a step size of 0.017° and 8 s counting time, in order to ensure sufficient resolution for structural refinement.

Fullprof Software was employed to carry out structural refinements from conventional XRD patterns using the Rietveld method. This method of refining the powder diffraction data was used to determine the crystal structure. Zero shift, lattice parameters, background, peak width, shape and asymmetry, atomic positions and isotropic temperature factors were all refined. The Thompson–Cox–Hastings pseudo-Voigt convoluted with axial divergence asymmetry function was used to describe the peak shape. Linear interpolation between set background points with refinable heights was used afterwards. The values were refined to improve the agreement factors.

All samples investigated by scanning electron microscopy (SEM) were first sputter-coated with Au in an EMITECH K550 apparatus. Field-emission scanning electron microscopy (FE-SEM) was performed using a JEM 6335F electron microscope with a field-emission gun operating at 10 kV. The FE-SEM was

also equipped with a LINK ISIS 300 detector for the energy-dispersive analysis of the X-rays (XEDS).

The specific surface area of the samples was determined by applying the BET method to nitrogen adsorption isotherms recorded at 77 K, using a Micrometrics apparatus model ASAP-2020. Prior to adsorption, the samples were degassed for 3 h at 110 °C.

High resolution transmission electron microscopy (HRTEM) analysis of the LCFCr powders was performed using a JEOL 3000F TEM, yielding an information limit of 1.1 Å. Images were recorded with an objective aperture of 70 µm, centered on a sample spot within the diffraction pattern area. Fast Fourier Transforms (FFTs) of the HRTEM images were carried out to reveal the periodic image contents using the Digital Micrograph package. The experimental HRTEM images were also compared to simulated images using MacTempas software. These computations were performed using information from the structural parameters, obtained from the Rietveld refinement, the microscope parameters, such as microscope operating voltage (300 kV) and spherical aberration coefficient (0.6 mm), and specimen parameters, such as zone axis and thickness. The defocus and sample thickness parameters were optimized by assessing the agreement between the model and the experimental data.

3. Results and discussion

3.1. Microwave-assisted synthesis of LCFCr powders: X-ray diffraction and Rietveld refinement

Fig. 1(a) shows the XRD patterns of the LCFCr powders synthesized by the combustion method (Method 1), as well as by microwave-assisted combustion (Method 2), and microwave-assisted sol–gel synthesis (Method 3). The diffraction patterns show that a pure crystalline phase is obtained for all three synthesis methods. Importantly, the temperature used did not exceed 1000 °C, and without the use of microwave methods, the normal temperature required to achieve the same result would be 1200 °C.

Fig. 1(b) shows the XRD patterns for the material synthesized by the microwave-assisted combustion method (Method 2) and calcined at three different temperatures. It can be seen that, at 700 °C, the phase is already forming and at 900 °C, the crystalline phase for LCFC has formed. Fig. 1(c) shows the XRD patterns for the material synthesized by the microwave-assisted sol–gel (Method 3) and calcined at the same temperatures. It can be seen that, at 700 °C and 900 °C, the desired phase is already forming and similar to Method 2, while at 1000 °C, the desired product is present in the pure form.

Fig. 2 shows the Rietveld refinement fits for the LCFCr samples produced by microwave-combustion method (Method 2, Fig. 1a) and synthesized by the microwave-assisted sol–gel synthesis (Method 3, Fig. 1b). The Rieltveld refinement for the LCFCr powders synthesized by the regular combustion method (Method 1) has been carried out in our parallel comparison studies [17]. A distorted perovskite structure with an orthorhombic symmetry (S.G. *Pnma*, 62) was confirmed for both samples. The unit cell vectors can be represented by $\sqrt{2}\boldsymbol{a}_p \times 2\boldsymbol{a}_p \times \sqrt{2}\boldsymbol{a}_p$, where $\boldsymbol{a}_p$ refers to the simple cubic perovskite cell. The results obtained for both samples concerning the cells parameters and the atomic positions are summarized in Table 1.

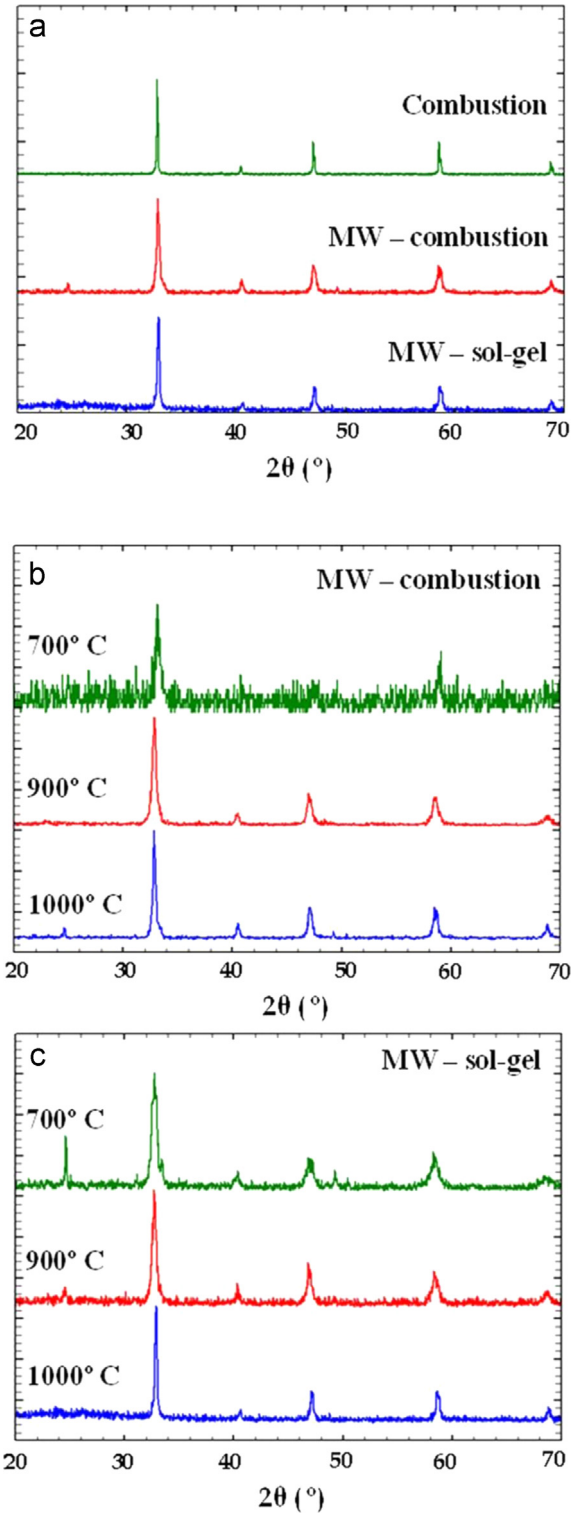

Fig. 1. Comparison of XRD patterns of LCFCr, synthesized by (a) the regular combustion method (Method 1) and two microwave-related methods, (b) by the microwave-combustion method (Method 2), and (c) by the microwave-assisted sol–gel method (Method 3) and calcined at three different temperatures, 700 °C (green), 900 °C (red) and 1000 °C (blue). (For interpretation of the references to color in this figure legend, the reader is referred to the web version of this article.)

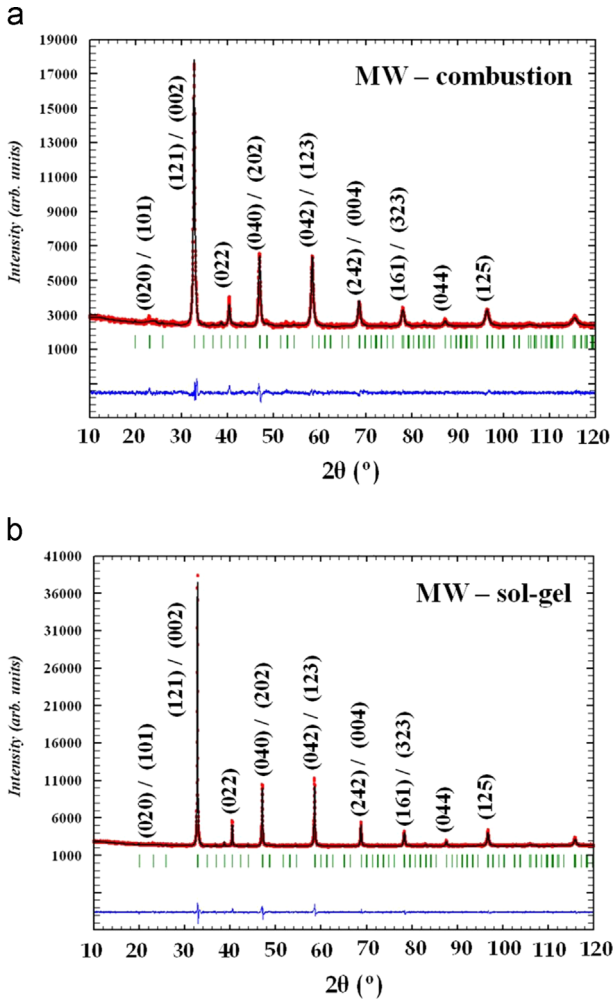

Fig. 2. Rietveld refinement of powder X ray diffraction patterns for LCFCr observed (red dotted lines), refined (black solid lines), and their difference (bottom line). Green vertical bars indicate the X-ray reflection positions. The patterns are for LCFCr powder (a) synthesized by the microwave-combustion method (Method 2) and (b) by the microwave-assisted sol–gel method (Method 3). (For interpretation of the references to color in this figure legend, the reader is referred to the web version of this article.)

Table 1
Structural parameters for LCFCr obtained from Rietveld refined XRD data.

	Conventional combustion (method 1)	LCFCr MW—combustion (method 2)	MW—sol–gel (method 3)
a **(Å)**	5.4540(2)	5.4615 (8)	5.4476(4)
b **(Å)**	7.7158(3)	7.7470 (7)	7.7194(2)
c **(Å)**	5.4544(1)	5.4619 (7)	5.4504(4)
La/Ca position 4c:			
X	0.0145(6)	0.01959 (7)	0.0151(6)
Z	−0.003(3)	−0.003 (1)	−0.0062(7)
Occ (La/Ca)	0.30(1)/0.70(1)	0.30(1)/0.70(1)	0.30(1)/0.70(1)
U***100 (Å^2)**	0.40(3)	0.44(4)	0.52(2)
Fe/Cr position 4b:			
Occ (Fe/Cr)	0.70(1)/0.30(1)	0.70(1)/0.30(1)	0.70(1)/0.30(1)
U***100 (Å^2)**	0.35(2)	0.32(3)	0.43(2)
O(1) position 4c:			
X	0.502(2)	0.503(4)	0.501(3)
Z	0.105(2)	0.106(4)	0.106(4)
Occ	1.00(1)	1.00(1)	1.00(1)
U***100 (Å^2)**	0.44(2)	0.27(3)	0.41(5)
O(2) position 8d:			
X	0.297(4)	0.256(2)	0.257(3)
Y	0.003(4)	0.005(3)	0.005(2)
Z	−0.254(3)	−0.31(2)	−0.30(3)
Occ	1.00(1)	1.00(1)	1.00(1)
U***100 (Å^2)**	0.33(2)	0.27(3)	0.41(5)
χ^2	0.96	1.58	1.74
R_{wp}/R_{exp} (%/%)	4.29/4.37	2.42/1.96	2.65/2.01
R_{Bragg}	4	3.83	5.11
S.G. *Pnma*: 4c (*x* 1/4 *z*), 4b (0 0 1/2), 8d (*xyz*)			

3.2. Microstructural analysis of LCFCr powders synthesized using microwave-assisted methods

Fig. 3 shows the SEM images of LCFCr powders formed using microwave-assisted combustion synthesis at 900 °C (Method 2, Fig. 3(a)) and microwave-assisted sol–gel synthesis and (Method 3, Fig. 3(b)). As can be seen, in both cases, the material has a porous morphology, which makes it a good candidate as an electrode material. A sponge-like porous morphology can be observed for the powders formed using Method 2 (Fig. 3(a)), which is the typical morphology found after combustion processes. The sponge-like porous morphology from Method 2 is quite different from the morphology obtained using the sol–gel method (Method 3, Fig. 3(b)) which consists of quite homogeneous agglomerated particles (approximate size 400 nm).

Further characterization of the material obtained by microwave-assisted sol–gel synthesis (Method 3) at 1000 °C and microwave-assisted combustion synthesis at 900 °C (Method 2) was performed, with Table 2 giving the elemental analysis of the materials. Table 2 shows the atomic percentage of the cations in LCFCr. The second column of results corresponds to the microwave-assisted combustion synthesis (Method 2) and the third column corresponds to microwave-assisted sol–gel synthesis (Method 3). The atomic percentage observed by EDX is comparable to the theoretical values, based on the expected stoichiometry of our material ($La_{0.3}Ca_{0.7}Fe_{0.7}Cr_{0.3}O_{3-\delta}$).

According to S_{BET} data in Table 3, the sample synthetized by the regular combustion method (Method 1) has a specific surface area of 0.89 $m^2\ g^{-1}$ whereas the sample synthetized by microwave-assisted combustion synthesis (Method 2) has a specific surface area of 10.4 $m^2\ g^{-1}$. This data is consistent with the calcination temperatures, as the lower calcination temperatures (300 °C lower for the microwave-assisted combustion synthesis (Method 2) sample) should lead to higher surface areas. Note that relatively low surfaces areas are observed in both cases, as typically observed for samples of this type [18]. However, a ca. 10 times increase in surface area is achieved by microwave-assisted combustion synthesis.

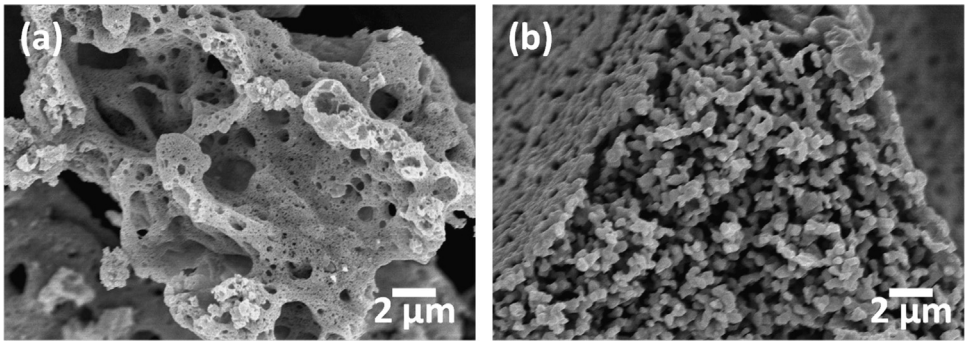

Fig. 3. SEM images of LCFCr powders formed using (a) microwave-assisted combustion synthesis (Method 2) and (b) microwave-assisted sol–gel synthesis (Method 3).

Table 2
EDX-determined composition (atomic %) of LCFCr powders, formed by microwave-assisted combustion (Method 2) and microwave-assisted sol–gel synthesis (Method 3) approaches.

Atomic % composition of $La_{0.3}Ca_{0.7}Fe_{0.7}Cr_{0.3}O_{3-\delta}$			
	MW and comb	**MW and sol–gel**	**Theoretical**
La	16 ± 0.5	16 ± 0.5	15
Ca	35 ± 0.5	34 ± 0.5	35
Cr	15 ± 0.5	15 ± 0.5	15
Fe	34 ± 0.5	36 ± 0.5	35

Table 3
Specific surface areas of LCFCr powders, formed by regular combustion (Method 1) and microwave-assisted combustion (Method 2) approaches.

Sample	S_{BET} ($m^2\ g^{-1}$)
Regular combustion (Method 1)	0.89
Microwave-assisted combustion (Method 2)	10.4

Transmission Electron Microscopy analysis was also performed on the LCFCr powder obtained using the different synthetic methods described above. The cation composition, measured semi-quantitatively by X-ray energy dispersive spectroscopy in more than ten single crystals, is in good agreement with the theoretical proportions in $La_{0.3}Ca_{0.7}Cr_{0.3}Fe_{0.7}O_{3-\delta}$, indicating the high purity of the powder.

In the HRTEM images of the crystals prepared by microwave-assisted combustion synthesis (Method 2) (Fig. 4a) and assisted sol–gel synthesis (Method 3) (Fig. 4b), nanosized twinned domains are seen. The appearance of these domains can be associated with the pseudo-cubic nature of these materials. Furthermore, their presence avoids the formation of tetrahedral chains and therefore the formation of undesired brownmillerite-type defects [19]. We have only detected the formation of defects in the sample prepared by sol–gel synthesis, Method 3 (Fig. 4b), showing a periodicity of 1.12 nm. This corresponds to the c axis of the $A_3B_3O_8$ type structure, which results from the intergrowth of a perovskite ABO_3 and a brownmillerite phase. HTREM images of the crystals prepared by the regular combustion method (Method 1) are shown in our parallel electrochemical study [17]. It is worth noting that the microwave-assisted combustion synthesis (Method 2), as it involves very fast processes, favors disordered phases (perovskite in our case).

4. Conclusions

The mixed ion–electron conducting perovskite, $La_{0.3}Ca_{0.7}Fe_{0.7}Cr_{0.3}O_{3-\delta}$ (LCFCr), was prepared here by using several microwave-assisted methods, for the ultimate use as a cathode in solid oxide fuel cells (SOFCs). The material was successfully prepared by microwave-assisted combustion (Method 2) and microwave-assisted sol–gel synthesis (Method 3). The desired product was obtained in crystalline form in only 7 hrs (vs. 13 h) and the synthesis temperature was roughly 300 °C lower than what is required for conventional solid-state combustion synthesis. This new approach has enhanced the rate of formation of the LCFCr powder and significantly increased the specific surface area from 0.89 to 10.4 $m^2\ g^{-1}$. These results are very encouraging, as they suggest that microwave synthesis can be used in the preparation of the perovskite materials used in our work. Whether the microwave-synthesized materials will give superior electrochemical performance is currently under investigation. It is suggested here that the partial substitution of Ca for Sr may promote oxygen-vacancy disordering and thus stabilize the perovskite phase vs. the brownmillerite phase. In our HRTEM work, the formation of brownmillerite-type defects was detected only in the sample prepared by sol–gel synthesis (Method 3). In addition, the calcination temperature for microwave-assisted combustion (Method 2) was 900 °C vs. 1000 °C for microwave-assisted sol–gel synthesis (Method 3). Based on the lower calcination temperature and the absence of brownmillerite-type defects, microwave-assisted combustion (Method 2) would likely be the preferred method for the future synthesis of highly active SOFC cathodes composed of the $La_{0.3}Ca_{0.7}Fe_{0.7}Cr_{0.3}O_{3-\delta}$ material.

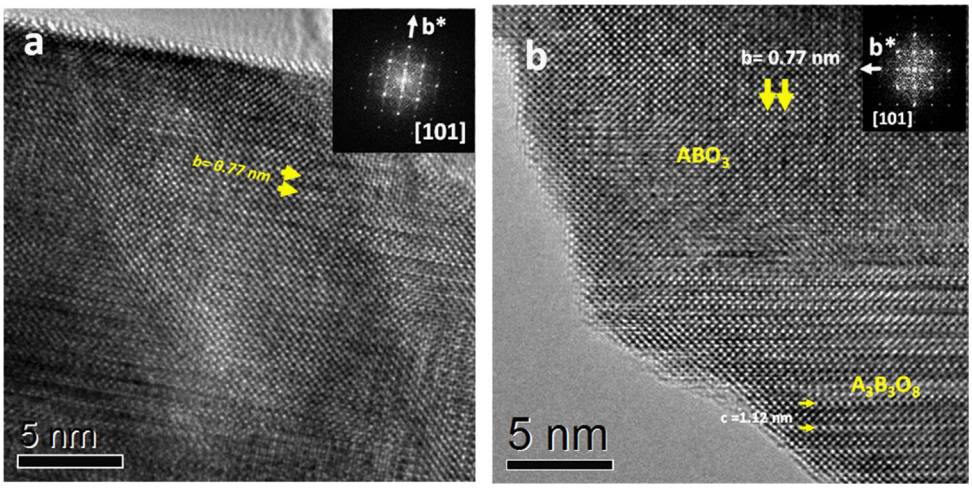

Fig. 4. HRTEM images of LCFCr crystals along the [1 0 1] zone axis and the corresponding diffraction patterns for powders formed by (a) microwave-assisted combustion synthesis (Method 2) and (b) microwave-assisted sol–gel synthesis (Method 3).

Acknowledgments

The authors are grateful to the Ministerio de Economía y Competitividad (Spain) and Comunidad de Madrid for the funding of projects MAT2013-64452-C4-4R and S2009/MIT-2753, respectively. J.P-G. also acknowledges the Universidad Complutense de Madrid for PhD scholarship support. We are also grateful to the Natural Sciences and Engineering Research Council of Canada (NSERC) Solid Oxide Fuel Cell Canada Strategic Research Network, as well as Carbon Management Canada (a Canadian National Centre of Excellence) for the support of this work.

References

[1] J. Prado-Gonjal, R. Schmidt, J.-J. Romero, D. Ávila, U. Amador, E. Morán, Microwave-assisted synthesis, microstructure, and physical properties of rare-earth chromites, Inorg. Chem. 52 (2012) 313–320.

[2] H.J. Kitchen, S.R. Vallance, J.L. Kennedy, N. Tapia-Ruiz, L. Carassiti, A. Harrison, A.G. Whittaker, T.D. Drysdale, S.W. Kingman, D. H. Gregory, Modern microwave methods in solid-state inorganic materials chemistry: from fundamentals to manufacturing, Chem. Rev. 114 (2013) 1170–1206.

[3] J. Lu, Y.-M. Yin, Z.-F. Ma, Preparation and characterization of new cobalt-free cathode $Pr_{0.5}Sr_{0.5}Fe_{0.8}Cu_{0.2}O_{3-\delta}$ for IT-SOFC, Int. J. Hydrog. Energy 38 (2013) 10527–10533.

[4] Q. Zhou, L. Xu, Y. Guo, D. Jia, Y. Li, W.C.J. Wei, $La_{0.6}Sr_{0.4}Fe_{0.8}Cu_{0.2}O_{3-\delta}$ perovskite oxide as cathode for IT-SOFC, Int. J. Hydrog. Energy 37 (2012) 11963–11968.

[5] L. Zhao, B. He, X. Zhang, R. Peng, G. Meng, X. Liu, Electrochemical performance of novel cobalt-free oxide $Ba_{0.5}Sr_{0.5}Fe_{0.8}Cu_{0.2}O_{3-\delta}$ for solid oxide fuel cell cathode, J. Power Sources 195 (2010) 1859–1861.

[6] A. Egger, E. Bucher, M. Yang, W. Sitte, Comparison of oxygen exchange kinetics of the IT-SOFC cathode materials $La_{0.5}Sr_{0.5}CoO_{3-d}$ and $La_{0.6}Sr_{0.4}CoO_3$, Solid State Ionics 225 (2012) 55–60.

[7] M. Chen, S. Paulson, V. Thangadurai, V. Birss, Sr-rich chromium ferrites as symmetrical solid oxide fuel cell electrodes, J. Power Sources 236 (2013) 68–79.

[8] J. Prado-Gonjal, B. Molero-Sánchez, D. Ávila-Brande, E. Morán, J. C. Pérez-Flores, A. Kuhn, F. García-Alvarado, The intercalation chemistry of H2V3O8 nanobelts synthesised by a green, fast and cost-effective procedure, J. Power Sources 232 (2013) 173–180.

[9] J. Prado-Gonjal, R. Morán, E. Microwave-Assisted, in: J. Zhang, H. Li (Eds.), Synthesis and characterization of perovskite oxides, in: Perovskite: Crystallography, Chemistry and Catalytic Performance, Nova Science Pub Incorporated, 2012, pp. 117–140 in.

[10] M. Gupta, W.W. Leong, Eugene, Microwaves and Metals, Wiley, 2008, p. 228 p.

[11] J.Y. Zhao, W., Microwave-assisted inorganic syntheses, in: E. Amsterdam (Ed.), Modern Inorganic Synthetic Chemistry, 2011, pp. 173–195.

[12] K.J. Rao, B. Vaidhyanathan, M. Ganguli, P.A. Ramakrishnan, Synthesis of inorganic solids using microwaves, Chem. Mater. 11 (1999) 882–895.

[13] S.D. Hutagalung, M.I.M. Ibrahim, Z.A. Ahmad, Microwave assisted sintering of $CaCu_3Ti_4O_{12}$, Ceram. Int. 34 (2008) 939–942.

[14] V.V. Kharton, A.V. Kovalevsky, M.V. Patrakeev, E.V. Tsipis, A. P. Viskup, V.A. Kolotygin, A.A. Yaremchenko, A.L. Shaula, E. A. Kiselev, J.o.C. Waerenborgh, Oxygen nonstoichiometry, mixed conductivity, and mössbauer spectra of $Ln_{0.5}A_{0.5}FeO_{3-\delta}$ (Ln = La − Sm, A = Sr, Ba): effects of cation size, Chem. Mater. 20 (2008) 6457–6467.

[15] J.-C. Grenier,M. Pouchard, P. Hagenmuller, Vacancy ordering in oxygen-deficient perovskite-related ferrites, in: Ferrites Transitions Elements Luminescence, Structure and Bonding 1981, pp. 1–25.

[16] B. Molero-Sánchez, P. Addo, M. Chen, S. Paulson, V. Birss, $La_{0.3}Ca_{0.7}Fe_{0.7}Cr_{0.3}O_{3-\delta}$ as a novel air electrode material for solid oxide electrolysis cells, in: 11th European SOFC & SOE FORUM 2014, Luzern, Switzerland, 2014.

[17] B. Molero-Sánchez, J. Prado-Gonjal, D. Ávila-Brande, M. Chen, E. Morán, V. Birss, High performance $La_{0.3}Ca_{0.7}Cr_{0.3}Fe_{0.7}O_{3-\delta}$ air electrode for reversible solid oxide fuel cell applications, Int. J. Hydrog. Energy 40 (2015) 1902–1910.

[18] K. Rida, A. Benabbas, F. Bouremmad, M.A. Peña, E. Sastre, A. Martínez-Arias, Effect of calcination temperature on the structural characteristics and catalytic activity for propene combustion of sol–gel derived lanthanum chromite perovskite, Appl. Catal., A: Gen. 327 (2007) 173–179.

[19] S.V. Rompaey, W. Dachraoui, S. Turner, O.Y. Podyacheva, H. Tan, J. Verbeeck, A. Abakumov, J. Hadermann, Layered oxygen vacancy ordering in Nb-doped $SrCo_{1-x} \times O$ 3 d, Z. Kristallogr 228 (2013) 28–34.